Chemical Physics Letters 833 (2023) 140948

Contents lists available at ScienceDirect

Chemical Physics Letters

journal homepage: www.elsevier.com/locate/cplett

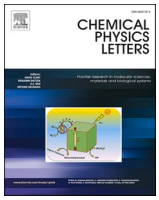

Preparation of ZnO/Ag nanoflowers by hydrothermal assisted with galvanic effect and its surface enhanced Raman scattering activity

Thi Ha Tran [a], Nguyen Hai Pham [b], Thi Huyen Nguyen [b], Thi Dieu Thu Nguyen [a], Cong Doanh Sai [b], Quang Hoa Nguyen [b], Viet Tuyen Nguyen [b,*], Minh Phuong Le [b], Van Tan Tran [b], Thanh Binh Nguyen [b], Trong Tam Nguyen [c], Thi Nguyet Duong [d], Tien Dat Tran [b], Ngoc Do Dai [b], Van Thanh Pham [b], An Bang Ngac [b,*]

[a] Hanoi University of Mining and Geology, Duc Thang, Tu Liem, Hanoi, Vietnam
[b] Faculty of Physics, VNU University of Science, Vietnam National University, Hanoi, 334 Nguyen Trai, Thanh Xuan, Hanoi, Vietnam
[c] Department of Physics, Faculty of Basic – Fundamental Sciences, Vietnam Maritime University, 484 Lach Tray, Le Tran District, Hai Phong, Vietnam
[d] Tran Nguyen Han High School, An Duong, Le Chan, Hai Phong, Vietnam

ARTICLE INFO

Keywords:
ZnO nanoflowers
Hydrothermal
Galvanic effect
Sputtering
Surface enhanced Raman scattering

ABSTRACT

An effective approach is proposed for fabrication of ZnO/Ag nanocomposite for surface enhanced Raman scattering application by combining hydrothermal assisted with galvanic effect and sputtering process. The sputtering process is applied to distribute Ag on the surface of ZnO nanostructures. The morphology, structure, elemental composition and optical properties of the samples were studied. The most suitable sputtering condition was identified to achieve the highest Raman enhancement. The optimum sputtering time of 70 s provides strong Raman signal of methylene blue, and demonstrates the potential of using the ZnO/Ag nanoflowers as sensitive surface enhanced Raman substrates.

1. Introduction

ZnO is one of the most well studied materials so far due to its attractive properties such as wide direct bandgap of 3.37 eV at room temperature, chemical and mechanical stability, and piezo electric effect, etc. These valuable and advanced properties of ZnO is further enhanced when the material is prepared in a various nano-forms such as nanoparticles [1–3], nanowires [4–6], nanorods [7–10], nanodisks [11,12], nano whiskers [13,14], tetra-pods [15,16] and more. These ZnO materials with different morphologies and structures offer a range of applications in electronics, opto-electronics, biomedicine, environment, etc.

Surface enhanced Raman scattering (SERS) has become an attractive method for detection of pollutants at low concentration [17–19]. Previous studies have demonstrated that Ag–ZnO [20–22] or Au–ZnO [9,23–26] hybrid nanostructures are active surface enhanced Raman scattering (SERS) substrates. However, the synthesis process of hybrid ZnO 1D nanostructures and noble metal nanostructures is complex and time consuming. In this paper, we introduce a facile method for fabricating sensitive SERS substrates based on Ag/ZnO nanoflowers in a short time without further treatment. ZnO nanoflowers were prepared by a hydrothermal process assisted with galvanic effect to improve the growth rate and density of ZnO nanostructures. By optimizing morphology of ZnO nanostructures and the sputtering time of silver, methylene blue (MB) at low concentration of 10^{-9} M was easily detected by Raman measurement with a short acquisition time.

2. Experiment

ZnO nanorods were prepared by galvanic effect assisted hydrothermal method. In a typical process, printed circuit board (PCBs) were thoroughly cleaned with distilled water, ethanol and acetone. The substrates were sonicated in HCl 5 % to remove the cupric oxide layer on the surface and then rinsed again with distilled water and dried by using nitrogen gun. The PCBs was covered with aluminum foil with an open area at the center. A galvanic cell structure between copper layer on PCBs and aluminum help to enhance the growth of ZnO nanorods. The as-prepared PCBs substrates were transferred to the hydrothermal reaction. The hydrothermal synthesis of ZnO nanorods was performed by suspending the as-produced ZnO wafers in a mixture of equimolar

* Corresponding authors.
E-mail addresses: nguyenviettuyen@hus.edu.vn (V.T. Nguyen), ngacanbang@hus.edu.vn (A.B. Ngac).

https://doi.org/10.1016/j.cplett.2023.140948
Received 11 October 2023; Received in revised form 7 November 2023; Accepted 8 November 2023
Available online 11 November 2023

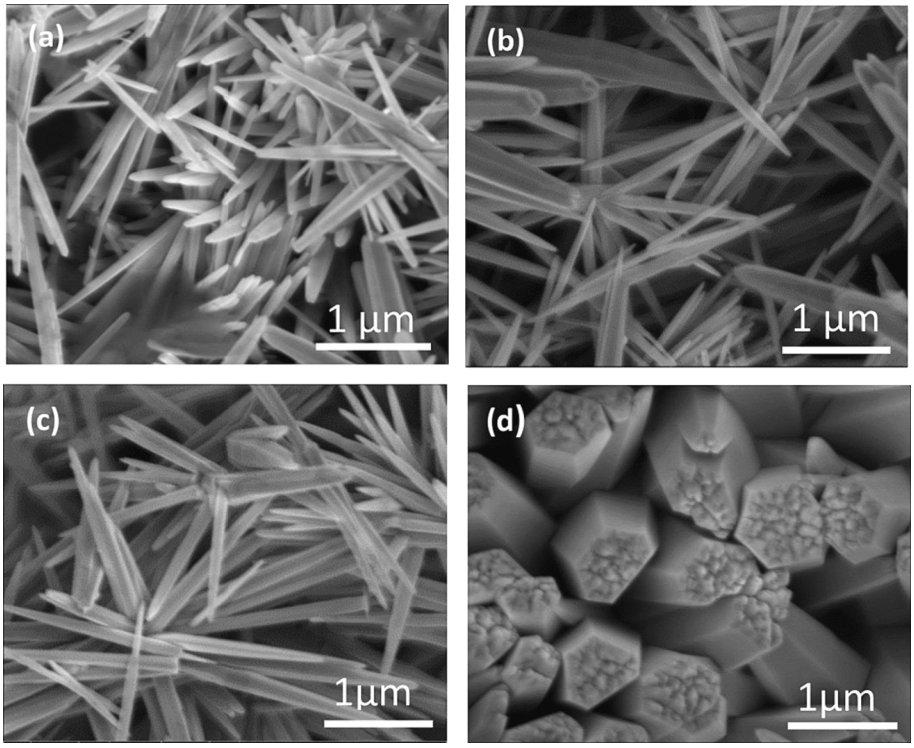

Fig. 1. SEM images of ZnO nanoflowers prepared with different precursor concentrations: 20 mM (a), 40 mM (b), 50 mM (c), 80 mM (d).

solution of zinc nitrate hexahydrate ($Zn(NO_3)_2{\cdot}6H_2O$) and hexamethylenetetramine ($C_6H_{12}N_4$) under continuous stirring. The growth temperature and time were set at 90 °C and 5 h, respectively.

After the growth process, the samples were rinsed with distilled water and dried. Structure of the products was studied by Xray diffractometer PANanalytical with monochromatic wavelength $\lambda = 1.54056$ Å of Cu-K_α radiation. The surface morphology of the samples was investigated using scanning electron microscope (NanoSEM Fei 450). Elemental composition of the samples was studied by using Energy Dispersive X-ray spectrometer integrated into the Scanning Electron Microscope.

Methylene Blue was used as Raman probe to study the Surface enhanced Raman scattering activity of the samples. Raman spectra were collected on Horiba Labram HR800 micro Raman system with excitation wavelength line 632.8 nm of He - Ne laser. The laser power was fixed at 0.5 mW on the surface samples in all measurements to prevent laser induced heating in SERS experiment.

3. Results and discussion

We first investigated the effect of zinc nitrate concentration on the morphology and structures of ZnO nanostructures produced by hydrothermal assisted with galvanic effect. Fig. 1 shows SEM images of ZnO nanostructures prepared by hydrothermal assisted with galvanic effect at different zinc nitrate concentrations of 20, 40, 50 and 80 mM.

The concentration of zinc salt in the precursor solution has a clear effect on the growth of ZnO nanoflowers. At concentrations of 20 mM and 40 mM, the obtained nanoproducts are formed at low density. At a concentration of 50 mM, ZnO nanoflowers grew more uniformly. Increasing of the zinc salt concentration to 80 mM transforms the flower-like ZnO nanostructures into thick rods with diameter of about 1 µm. The results can be understood that at high concentration, the crystal growth rate is higher and leads to formation of bigger rods. The fact that these small diameter nanorods tends to merge together to form larger rods can be understood as these structures possess smaller surface energy. However, these structures possess lower specific surface area and

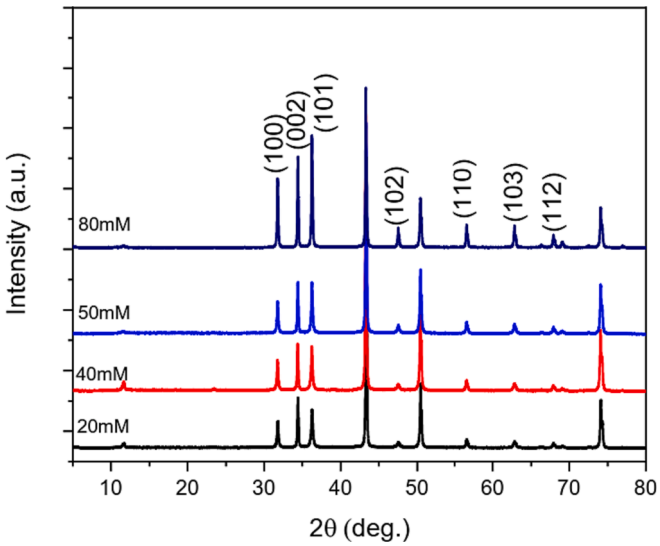

Fig. 2. XRD diffraction patterns of ZnO nanoproducts prepared with different concentration of precursor concentrations.

might limit the efficiency of Raman enhancement. Taking this effect into account, the sample prepared with precursor concentration of 50 mM was studied further for SERS application. It can be seen that precursor concentration of 50 mM offers homogenous products of nanoflowers. Fig. 1c shows that ZnO nanorods grow radially from a single core to form flower structure. The obtained nanoproducts are uniform in both size and shape. The results clearly show the advantages of galvanic technique on the growth of uniform ZnO nanostructures, which is critical to the reproducibility of Raman signal on SERS substrate based on the as-prepared ZnO nanoproducts.

The X-ray diffraction (XRD) studies were carried out to analyze the crystal structure and purity of the ZnO nanoflower as a function of the

Table 1
Lattice parameters and crystallite size of the produced ZnO nanostructures with different precursor concentrations.

Precursor concentration	Lattice parameters a (Å)	b (Å)	c (Å)
20 mM	3.251	3.251	5.210
40 mM	3.252	3.252	5.207
50 mM	3.250	3.250	5.210
80 mM	3.250	3.250	5.200

synthesis conditions. XRD patterns of the obtained ZnO nanostructures are shown in Fig. 2. The XRD patterns show clear diffraction peaks at 31.55°; 34.41°; 36.25°; 47.44°; 56.66°; 63.11°; 68.16°, which can be identified as the reflection from (100), (002), (101), (102), (110), (103), (112) planes of hexagonal wurtzite structure of ZnO (JCPDS 79-0207). The high intensity of these peaks along with absence of peaks related to impurities in the patterns imply that the obtained ZnO materials showed excellent crystallinity. The lattice parameters and crystallite sizes of the ZnO nanoproducts estimated by using the Scherrer equation are given in Table 1. The estimated lattice parameters of all the samples are in good agreement with those reported for ZnO materials [27,28]. XRD analysis of the as-synthesized ZnO nanoflowers at different zinc salt concentrations showed an increased in peak intensities, showing that the zinc salt concentration is an important factor in enhancing the crystallinity of the samples. The preferred growth orientation was not observed in the XRD patterns of the prepared samples. This result can be explained as the ZnO nanorods spread out in random directions to form ZnO nanoflowers.

Fig. 3 shows a typical EDS spectrum of ZnO nanoflowers obtained with precursor concentration of 50 mM. The EDS data reconfirms the purity of the products as no other element besides Zn, O, and Cu could be observed. It should be noted that the signal of Cu element comes from the PCBs substrate used in this research.

The Raman spectra of the as-grown ZnO nanoproducts prepared with different concentration of precursors are displayed in Fig. 4. Raman peaks at 99, 202; 330; 376; 437 cm^{-1} corresponds to the vibration modes E_{2low}; $2E_2$ (low); E_{2H}-E_{2L}; $A_{1(TO)}$ and E_{2high}, respectively [29,30]. The two most prominent peaks at 99 and 437 cm^{-1} are related to the vibration of oxygen and zinc lattices, respectively [10,30]. The appearance of peaks such as 215 and 333 cm^{-1} as well as high background associated with internal defects such as oxygen vacancies, zinc interstitial and others [31] in the spectrum of samples prepared at concentrations 20 and 80 mM showed that the crystal quality was not as good as the samples prepared at 50 mM concentrations. The results suggest that the sample obtained with precursor concentration of 50 mM is of highest uniform and quality, which is suitable for SERS application and was further investigated.

The obtained ZnO nanoflowers were then sputtered with Ag. SEM image of the sample is displayed in Fig. 5a. The image shows that Ag is evenly distributed on the surface of ZnO nanoflowers. EDS spectrum of ZnO/Ag sample in Fig. 5b shows clear trace of Ag element. The result was reconfirmed by the XRD diffraction pattern (Fig. 5c). As shown in Fig. 5c, the presence of cubic phase of metallic Ag (JCPDF = 893722) is clearly visible at 38.19°; 45.9°; 66.89°; 76.98° corresponding to the reflection from (111), (200), (220), (311) planes.

Subsequently, we evaluated SERS activity of ZnO/Ag nanoflowers, using Methylene Blue as Raman probe. Fig. 6 shows SERS spectra of MB adsorbed on ZnO/Ag nanorods prepared with different sputtering times. The most prominent peaks around 1621 cm^{-1} can be attributed to C–C ring stretching, bands above 1396 cm^{-1} to the CH in plane deformation, the bands at 1042 cm^{-1} to CH in-plane bending modes [32]. The highest enhancement and uniformity were achieved for the sample prepared with sputtering time of 70 s. This is explained because, at the Ag sputtering time of less than 70 s, the density of Ag nanoparticles is low. However, if the sputtering time is increased to 140 s, it is possible to

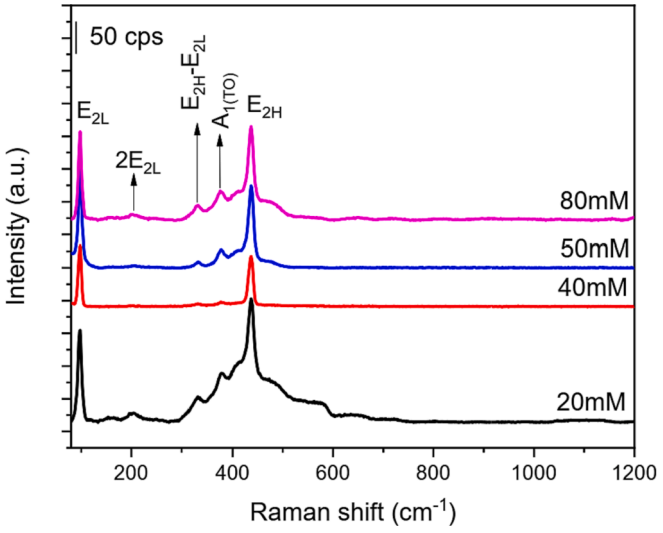

Fig. 4. Raman spectra of samples prepared with different precursor concentrations.

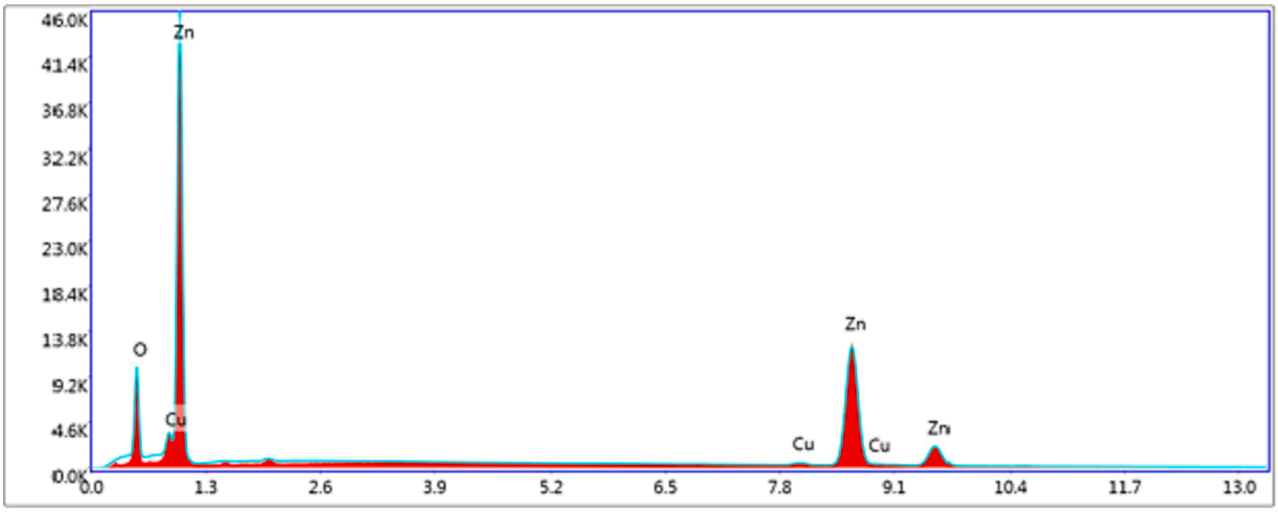

Fig. 3. EDS spectrum of ZnO nanoflowers prepared with zinc salt concentration of 50 mM.

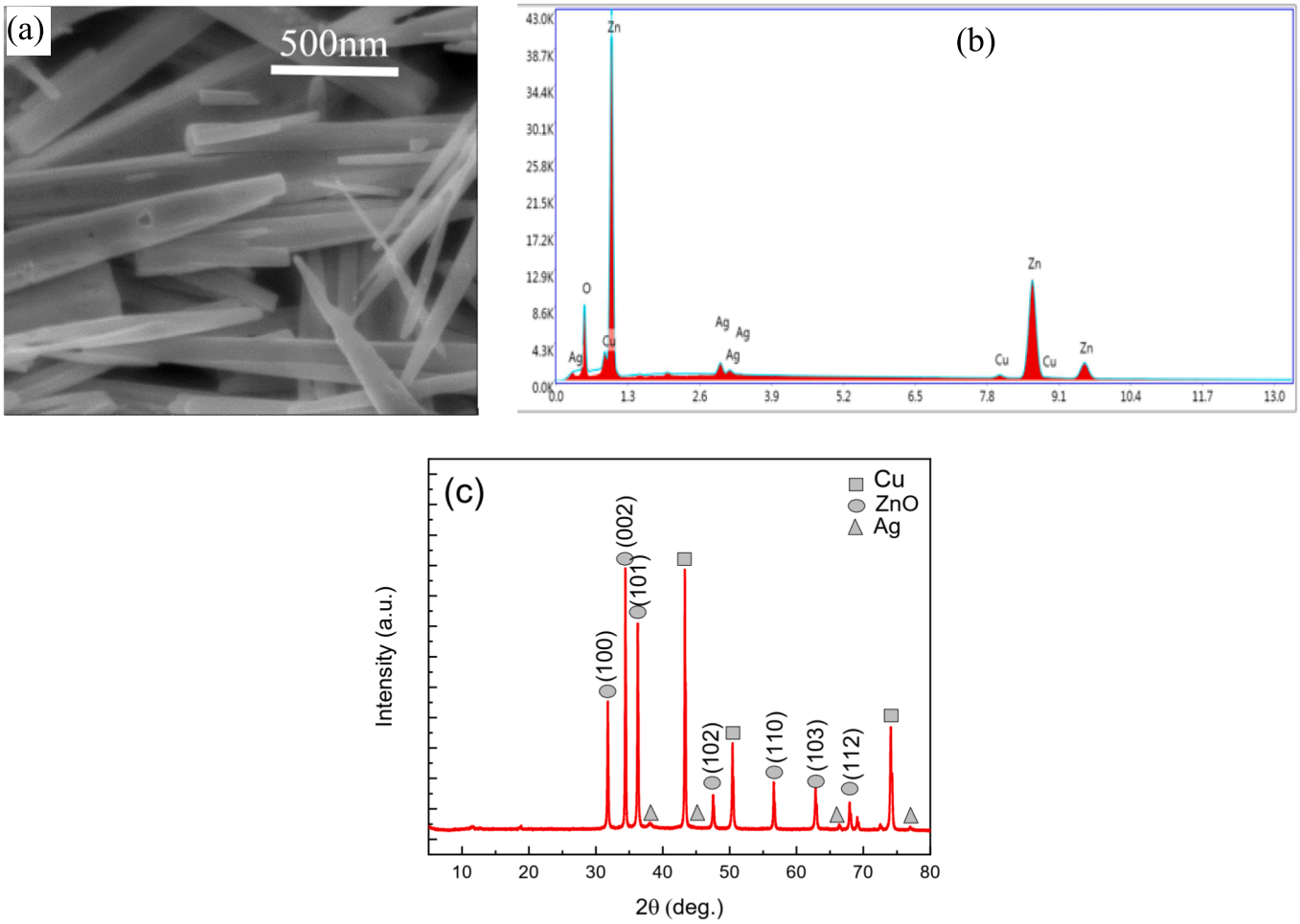

Fig. 5. SEM image (a); EDS spectrum (b) and XRD pattern of ZnO/Ag nanoflower prepared with sputtering time of 70 s.

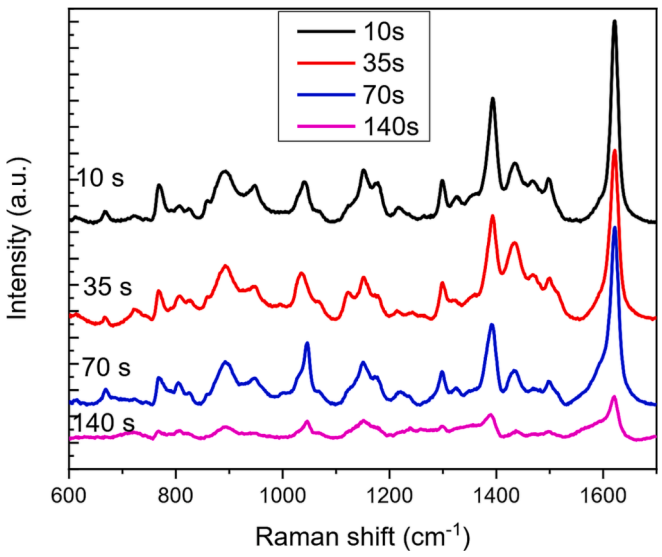

Fig. 6. Raman spectra of MB 10^{-8} M measured on ZnO/Ag prepared with different sputtering time: 10 s, 35 s, 70 s, 140 s.

create large islands and even continuous layer, limiting the formation of "hot spots".

Raman spectra of MB collected at 30 different points on the ZnO/Ag nanoflower substrates (Fig. 7a) were collected. The data showed that relative standard deviation (RSD) estimated for the peak at 1621 cm^{-1} was only 8.4 % (Fig. 7b). The low RSD of the prepared substrates suggested that ZnO/Ag nanoflowers can be used as a reliable SERS substrate to detect substances of low concentration. Fig. 7c shows Raman spectra of MB with concentration from 10^{-6} to 10^{-10} M on ZnO/Ag nanoflowers. It can be seen that the Raman intensity increases monotonically with MB concentration. Characteristic peaks of MB were observed clearly for concentration down to 10^{-9} M. However, SERS signal of MB almost diminished at concentration of 10^{-10} M. The results indicate the high sensitivity of the prepared SERS substrates.

The superiority of SERS substrates based on ZnO/Ag nanoflowers can be ascribed to several simultaneous phenomena. Firstly, the local plasmon resonance in Ag nanoparticles in charge of electromagnetic enhancement of Raman signal is significantly intensified due to the increased density of hot spots distributed on the surface of ZnO nanoflowers. This is made possible thanks to high surface area of nanomaterials. Secondly, hetero-junction between metal nanostructures and semiconductor nanomaterials further enhances electromagnetic field at the surface of metallic nanomaterials where Raman probes are located [10,26]. Furthermore, chemical enhancement via charge transfer between ZnO semiconductor and MB as well as between Ag nanoparticles and MB is also facilitated and contributes to the total enhancement of Raman signal [25].

4. Conclusion

The ZnO/Ag nanoflowers were successfully prepared by galvanic

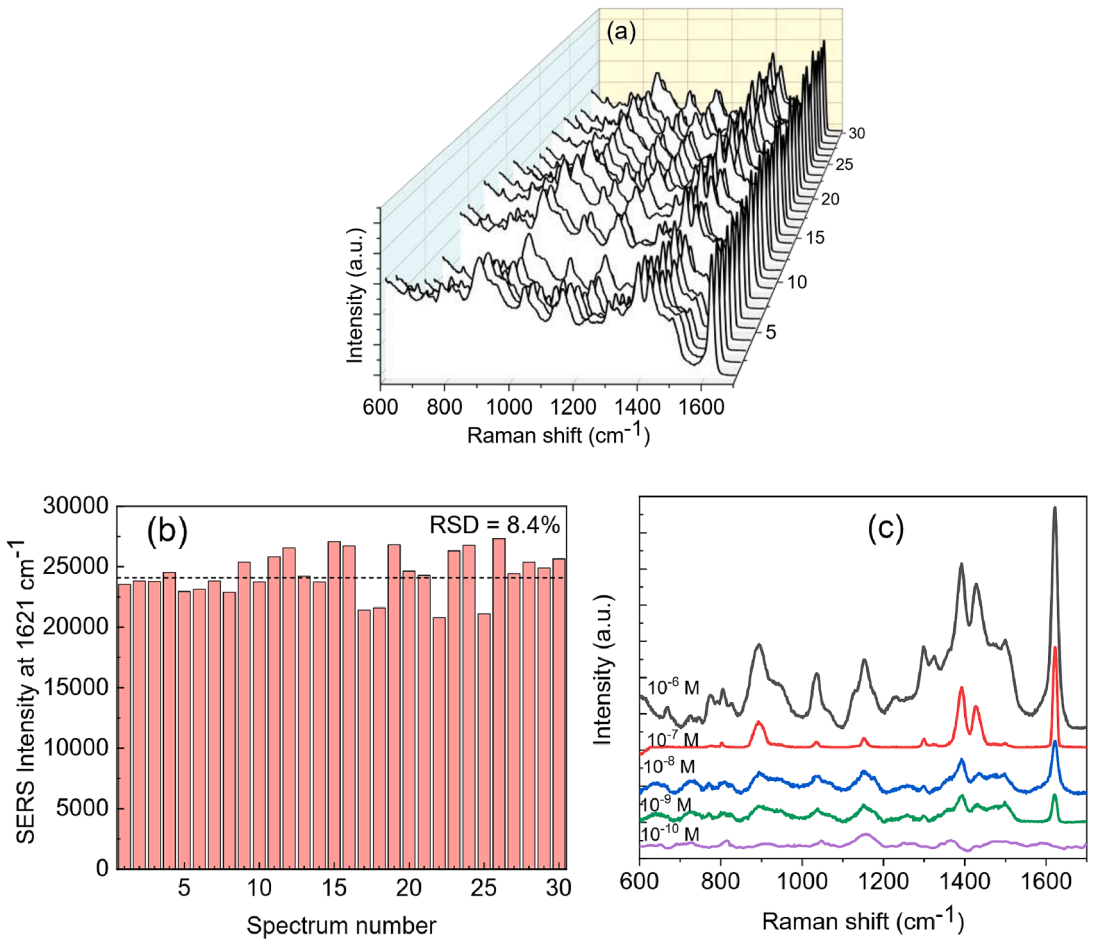

Fig. 7. (a) Raman spectra of MB collected at 30 randoms points on ZnO/Ag nanoflowers prepared with sputtering time of 70 s; (b) Relative standard deviation of specific Raman mode at 1621 cm^{-1} of 30 random points and (c) Raman spectra of MB at different concentrations measured on ZnO/Ag nanoflowers.

effect assisted hydrothermal method in combination with sputtering technique. Galvanic effects show beneficial effect on the growth of ZnO nanoflowers in term of higher density and more uniform morphology. The optimum sputtering time of 70 s offers high quality SERS substrate of high uniformity and sensitivity. The as-prepared structures are sensitive SERS substrates which was demonstrated by the detection of MB at low concentration of 10^{-9} M.

5. Author's contribution statement

Thi Ha Tran, Viet Tuyen Nguyen conceived of the presented idea.

Thi Huyen Nguyen, Van Tan Tran and Minh Phuong Le prepared the sample under supervision of Thi Ha Tran.

Thi Huyen Nguyen, Van Tan Tran, Minh Phuong Le, Cong Doanh Sai, Quang Hoa Nguyen, Thanh Binh Nguyen, Trong Tam Nguyen, Thi Nguyet Duong, Tien Dat Tran, Ngoc Do Dai, Thi Dieu Thu Nguyen, Van Thanh Pham carried out experiment.

Thi Ha Tran wrote the manuscript.

Thi Ha Tran, Nguyen Hai Pham, Van Thanh Pham, An Bang Ngac contributed to the interpretation of the results.

Nguyen Hai Pham, An Bang Ngac and Viet Tuyen Nguyen proofread the manuscript.

All authors discussed the results and contributed to the final manuscript.

Declaration of Competing Interest

The authors declare that they have no known competing financial interests or personal relationships that could have appeared to influence the work reported in this paper.

Data availability

Data will be made available on request.

Acknowledgements

This research is funded by the Vietnam Ministry of Education and Training under grant number B2023-MDA-01. Ms. Minh Phuong Le was funded by the Master, PhD Scholarship Programme of Vingroup Innovation Foundation (VINIF), code VINIF.2023.ThS.108.

References

[1] S. Anjum, M. Hashim, S.A. Malik, M. Khan, J.M. Lorenzo, B.H. Abbasi, C. Hano, Recent advances in zinc oxide nanoparticles (ZnO NPs) for cancer diagnosis, target drug delivery, and treatment, Cancers (basel) 13 (2021) 4570, https://doi.org/10.3390/CANCERS13184570.

[2] C. Pushpalatha, J. Suresh, V.S. Gayathri, S.V. Sowmya, D. Augustine, A. Alamoudi, B. Zidane, N.H. Mohammad Albar, S. Patil, Zinc oxide nanoparticles: a review on its applications in dentistry, Front. Bioeng. Biotechnol. 10 (2022), 917990, https://doi.org/10.3389/fbioe.2022.917990.

[3] T.D. Canh, N.V. Tuyen, N.N. Long, Influence of solvents on the growth of zinc oxide nanoparticles fabricated by microwave irradiation, VNU J. Sci. Math. Phys. 25 (2009) 71–76.

[4] K. Yoo, W. Lee, K. Kang, I. Kim, D. Kang, D.K. Oh, M.C. Kim, H. Choi, K. Kim, M. Kim, J.D. Kim, I. Park, J.G. Ok, Low-temperature large-area fabrication of ZnO nanowires on flexible plastic substrates by solution-processible metal-seeded hydrothermal growth, Nano Converg. 7 (2020) 1–10, https://doi.org/10.1186/S40580-020-00235-6/FIGURES/11.

[5] X. Zhao, K. Nagashima, G. Zhang, T. Hosomi, H. Yoshida, Y. Akihiro, M. Kanai, W. Mizukami, Z. Zhu, T. Takahashi, M. Suzuki, B. Samransuksamer, G. Meng, T. Yasui, Y. Aoki, Y. Baba, T. Yanagida, Synthesis of Monodispersedly Sized ZnO Nanowires from Randomly Sized Seeds, Nano Lett. 20 (2020) 599–605, https://doi.org/10.1021/ACS.NANOLETT.9B04367/SUPPL_FILE/NL9B04367_SI_001.PDF.
[6] A. Galdámez-Martinez, G. Santana, F. Güell, P.R. Martínez-Alanis, A. Dutt, Photoluminescence of zno nanowires: A review, Nanomaterials 10 (2020) 857, https://doi.org/10.3390/nano10050857.
[7] P.K. Aspoukeh, A.A. Barzinjy, S.M. Hamad, Synthesis, properties and uses of ZnO nanorods: a mini review, International Nano Letters 2021 12:2. 12 (2021) 153–168. https://doi.org/10.1007/S40089-021-00349-7.
[8] N. Minh Nguyen, ad Duc Anh Ngo, bd Le Ngoc Thu Nguyen, bd Hoai Nhan Luong, bd Ha Ngoc Duy Huynh, bd Bui Gia Man Nguyen, bd Nhat Giang Doan, bd Le Thai Duy, bd Anh Vy Tran, ef Cong Khanh Tran, bd Kim Ngoc Pham bcd, V. Quang Dang, Developing low-cost nanohybrids of ZnO nanorods and multi-shaped silver nanoparticles for broadband photodetectors, RSC Adv. 13 (2023) 21703–21709. https://doi.org/10.1039/D3RA03485B.
[9] T.H. Tran, T.H.T. Nguyen, M.H. Nguyen, N.H. Pham, A.B. Ngac, H.H. Mai, V. T. Pham, T.B. Nguyen, K.H. Ho, T.T. Nguyen, V.T. Nguyen, Synthesis of ZnO/Au Nanorods for Self Cleaning Applications, J. Nanosci. Nanotechnol. 21 (2021) 2621–2625, https://doi.org/10.1166/jnn.2021.19110.
[10] V.T. Tran, T.H. Tran, M.P. Le, N.H. Pham, V.T. Nguyen, D.B. Do, X.T. Nguyen, B.N. Q. Trinh, T.T. Van Nguyen, V.T. Pham, M.Q. Luu, A.B. Ngac, Highly efficient photo-induced surface enhanced Raman spectroscopy from ZnO/Au nanorods, Opt. Mater. (amst) 134 (2022), 113069, https://doi.org/10.1016/j.optmat.2022.113069.
[11] M. Maruthupandy, T. Muneeswaran, G. Chackaravarthi, T. Vennila, M. Anand, W. S. Cho, F. Quero, Development of hexagonal ZnO nanodisks for potential catalytic reduction of p-nitrophenol, Mater. Chem. Phys. 285 (2022), 126145, https://doi.org/10.1016/J.MATCHEMPHYS.2022.126145.
[12] P.B. Jaiswal, S. Jejurikar, A. Mondal, B. Pushkar, S. Mazumdar, Antibacterial Effects of ZnO Nanodisks: Shape Effect of the Nanostructure on the Lethality in Escherichia coli, Appl. Biochem. Biotechnol. 195 (2023) 3067–3095, https://doi.org/10.1007/s12010-022-04265-0.
[13] H.B. Lin, M.S. Cao, J. Yuan, D.W. Wang, Q.L. Zhao, F.C. Wang, Enhanced mechanical behaviour of lead zirconate titanate piezoelectric composites incorporating zinc oxide nanowhiskers, Chin. Phys. B 17 (2008) 4323, https://doi.org/10.1088/1674-1056/17/11/060.
[14] I.D. Venevtsev, A.P. Tarasov, A.E. Muslimov, E.I. Gorokhova, L.A. Zadorozhnaya, P.A. Rodnyi, V.M. Kanevsky, Ultraviolet luminescence of zno whiskers, nanowalls, multipods, and ceramics as potential materials for fast scintillators, Materials 14 (2021) 1–13, https://doi.org/10.3390/ma14082001.
[15] D. Yang, R.A. Gopal, T. Lkhagvaa, D. Choi, Oxidizing agent impacting on growth of ZnO tetrapod nanostructures and its characterization, Environ. Res. 197 (2021), 111032, https://doi.org/10.1016/J.ENVRES.2021.111032.
[16] A. Knoepfel, N. Liu, Y. Hou, S. Sujani, B.R. dos Reis, R. White, K. Wang, B. Poudel, S. Gupta, S. Priya, Development of Tetrapod Zinc Oxide-Based UV Sensor for Precision Livestock Farming and Productivity, Biosensors (basel). 12 (2022) 837, https://doi.org/10.3390/bios12100837.
[17] M. Shao, C. Ji, J. Tan, B. Du, X. Zhao, J. Yu, B. Man, K. Xu, C. Zhang, Z. Li, Ferroelectrically modulate the Fermi level of graphene oxide to enhance SERS response, Opto-Electronic Adv. (2023) 230094. https://doi.org/10.29026/oea.2023.230094.
[18] S. Bai, X. Ren, K. Obata, Y. Ito, K. Sugioka, Label-free trace detection of biomolecules by liquid-interface assisted surface-enhanced Raman scattering using a microfluidic chip, Opto-Electronic Adv. 5 (2022). https://doi.org/10.29026/oea.2022.210121.
[19] Z. Pei, J. Li, C. Ji, J. Tan, Z. Shao, X. Zhao, Z. Li, B. Man, J. Yu, C. Zhang, Flexible Cascaded Wire-in-Cavity-in-Bowl Structure for High-Performance and Polydirectional Sensing of Contaminants in Microdroplets, J. Phys. Chem Lett. 14 (2023) 5932–5939, https://doi.org/10.1021/acs.jpclett.3c00988.
[20] L. Ma, Q. Zhang, J. Li, X. Lu, C. Gao, P. Song, L. Xia, Ag–ZnO Nanocomposites Are Used for SERS Substrates and Promote the Coupling Reaction of PATP, Materials. 14 (2021) 1–9, https://doi.org/10.3390/MA14040922.
[21] M.E. Koleva, N.N. Nedyalkov, R. Nikov, R. Nikov, G. Atanasova, D. Karashanova, V.I. Nuzhdin, V.F. Valeev, A.M. Rogov, A.L. Stepanov, Fabrication of Ag/ZnO nanostructures for SERS applications, Appl Surf Sci. 508 (2020), 145227, https://doi.org/10.1016/J.APSUSC.2019.145227.
[22] E. Ashok Kumar, N. Riswana Barveen, T.J. Wang, T. Kokulnathan, Y.H. Chang, Development of SERS platform based on ZnO multipods decorated with Ag nanospheres for detection of 4-nitrophenol and rhodamine 6G in real samples, Microchemical Journal. 170 (2021), 106660, https://doi.org/10.1016/J.MICROC.2021.106660.
[23] S. Kalasung, K. Aiempanakit, I. Chatnuntawech, N. Limsuwan, K. Lertborworn, V. Patthanasettakul, M. Horprathum, N. Nuntawong, P. Eiamchai, Trace-level detection and classifications of pentaerythritol tetranitrate via geometrically optimized film-based Au/ZnO SERS sensors, Sens Actuators B Chem. 366 (2022), 131986, https://doi.org/10.1016/J.SNB.2022.131986.
[24] S. Kalasung, I. Chatnuntawech, V. Patthanasettakul, S. Limwichean, K. Lertborworn, M. Horprathum, N. Nuntawong, P. Eiamchai, K. Aiempanakit, Au-decorated ZnO nanorod arrays for SERS-active substrates towards trace detection and classification of pentaerythritol tetranitrate, Mater Today Proc. 47 (2021) 3517–3524, https://doi.org/10.1016/J.MATPR.2021.03.511.
[25] T. Nguyen Viet, Preparation of ZnO nanoflowers for surface enhance Raman scattering applications, VNU Journal of Science: Mathematics -, Physics. 36 (2020) 1–6. https://doi.org/10.25073/2588-1124/vnumap.4369.
[26] Q.K. Doan, M.H. Nguyen, C.D. Sai, V.T. Pham, H.H. Mai, N.H. Pham, T.C. Bach, V. T. Nguyen, T.T. Nguyen, K.H. Ho, T.H. Tran, Enhanced optical properties of ZnO nanorods decorated with gold nanoparticles for self cleaning surface enhanced Raman applications, Appl Surf Sci. 505 (2020), 144593, https://doi.org/10.1016/j.apsusc.2019.144593.
[27] H. Ennaceri, M. Boujnah, D. Erfurt, J. Rappich, X. Lifei, A. Khaldoun, A. Benyoussef, A. Ennaoui, A. Taleb, Influence of stress on the photocatalytic properties of sprayed ZnO thin films, Solar Energy Materials and Solar Cells. 201 (2019), 110058, https://doi.org/10.1016/J.SOLMAT.2019.110058.
[28] J. Liu, H. Liang, Heterogeneous nucleation and self-nucleation of isotactic polypropylene with addition of nano-ZnO, J Therm Anal Calorim. 146 (2021) 2115–2126, https://doi.org/10.1007/S10973-020-10446-Y/METRICS.
[29] S. Knust, L. Ruhm, A. Kuhlmann, D. Meinderink, J. Bürger, J.K.N. Lindner, M.T. de los Arcos de Pedro, G. Grundmeier, In situ backside Raman spectroscopy of zinc oxide nanorods in an atmospheric-pressure dielectric barrier discharge plasma, J. Raman Spectrosc. 52 (2021) 1237–1245. https://doi.org/10.1002/JRS.6123.
[30] T.M. Khan, T. Bibi, B. Hussain, Synthesis and optical study of heat-treated ZnO nanopowder for optoelectronic applications, Bull. Mater. Sci. 38 (2015) 1851–1858, https://doi.org/10.1007/S12034-015-1103-9/METRICS.
[31] S.H. Ribut, C.A. Che Abdullah, M.Z. Mohammad Yusoff, Investigations of structural and optical properties of zinc oxide thin films growth on various substrates, Results Phys. 13 (2019), 102146, https://doi.org/10.1016/J.RINP.2019.02.082.
[32] C. Gu, S. Man, J. Tang, Q. Ye, Z. Yu, Preparation of silicon surface pyramid arrays and modification of thin gold film for surface-enhanced Raman scattering, IOP Conf. Ser. Mater. Sci. Eng. 394 (2018), 022049, https://doi.org/10.1088/1757-899X/394/2/022049.